JSEE Vol. 22, No. 4, 2020 DOI: 10.48303/jsee.2022.252303

Research Paper

Study of Seismic Performance of Self-Centering Steel Plate Shear Walls at DBE and MCE

Sorour Arjmandzadeh[1*] and Abdolreza S. Moghadam[2]

1. Ph.D. Candidate, International Institute of Earthquake Engineering and Seismology (IIEES), Tehran, Iran, *Corresponding Author; email: sorour.arjmand@gmail.com
2. Associate Professor, Structural Engineering Research Center, International Institute of Earthquake Engineering and Seismology (IIEES), Tehran, Iran

Received: 08/02/2022
Revised: 05/04/2022
Accepted: 23/05/2022

ABSTRACT

Self-Centering Steel Plate Shear Wall (SC-SPSW) is a promoted steel shear wall in which steel web plates absorb the seismic energy and Self-Centering connections bring the structure back to its original position after a ground motion. The main goals of this seismic resisting system are mitigating plastic damage in the mail structural elements such as beams and columns and reducing the residual drift after the earthquake. This paper offers a study to evaluate the efficiency of this innovative system in midrise buildings at Design Based Earthquake (DBE) and Maximum Credible Earthquake (MCE). Three archetypes which are five, seven and ten story office buildings are prepared to be representative of midrise buildings. Each archetype is designed to bear 4% gap opening at the connections. Infill plates alone can resist 100% of the specified seismic load without considering boundary frame moment resistance. Nonlinear dynamic analysis under a set of far-field ground motion consisting of seven records is performed to estimate the seismic performance of the archetypes. The results of the dynamic analysis consisting main structural damage, inter-story drift and residual drift are studied to assess the efficiency of Self-Centering Steel Plate Shear Wall. According to the analysis results, the residual drifts of all archetypes were significantly reduced and full self-centering was achieved at both DBE and MCE level. In addition, beams and columns demonstrated no plastic deformation in nonlinear dynamic analysis at DBE and MCE ground motion, which is a great achievement to keep the main structural element safe during the earthquake. Inter-story drift in the archetype was below the allowable amount suggested by seismic design code except for upper stories that could be improved by choosing proper thickness for upper web plates

Keywords:
Steel Plate Shear Wall; Self-centering; Post Tensioning; Residual Drift; Seismic Damage; Seismic Performance

1. Introduction

Conventional design codes, allow structural engineers to design buildings with the aim of predictable and ductile behavior in severe earthquakes, in order to prevent collapse and loss of life. However, some controlled damage is expected, which may result in the building being damaged beyond economic repair after severe shaking. In the recent decades a lot of effort has been made to promote the seismic performance of structures and decrease the damage during a ground motion.

One of the remarkable solutions to mitigate the seismic damage was proposed by Ricles et al. [1] for steel frames in which welded connection is replaced by post-tensioned connection. Since a gap opens between beam and column in the post-tensioned connection, no plastic hinge could be formed in the connection. Similar post-tensioned connection was studied by Christopoulos et al. [2] for precast

concrete.

Post-tensioned connection has been studied numerically and experimentally in association with different type of energy dissipating system. A slightly different post-tensioned connection in steel frame proposed by Garlock et al. [3] in which energy dissipation is provided by bolted steel top and seat angles where hysteretic energy is dissipated through flexural plastic hinging of the angles.

A post-tensioned friction damped connection (PFDC), was proposed by Rojas et al. [4] that dissipates seismic energy by friction devices located at the top and bottom of the beam where a bolted connection is made to both the beam and column flanges.

A bottom flange friction device (BFFD) connection was proposed as an alternative to the PFDC connection by Iyama et al. [5] and Wolski et al. [6]. The proposed BFFD friction device is attached only to the beam bottom flange to avoid interference with the floor slab.

Lin et al. [7] investigated beam web friction devices (WFDs) to provide energy dissipation that consist of two channel sections welded to the column. These friction channels are bolted to the beam web with brass cartridge plates sandwiched between the web and the channel to provide friction.

Clayton [8] investigated the behavior of post-tensioned connection paired with steel web plates entitled as Self-Centering Steel Plate Shear Wall (SC-SPSW) and offered a design method for this system. Experimental investigation of SC-SPSW firstly developed as a part of a research project funded by Network Earthquake Engineering Simulation, entitled "Smart and Resilient Steel Walls for Reducing Earthquake Impacts". Part of the experiments was accomplished by Clayton [9] at the University of Washington and Dowden [10] at the University of Buffalo. Arjmandzadeh and Moghadam [11] studied the numerical simulation of Self-Centering Steel Plate Shear Wall using the results of the test specimen conducted by Dowden. Damage-resistant design is developing rapidly, in several different forms. These include rocking walls or rocking frames, with or without post-tensioning, and a variety of energy dissipating devices attached to the building in different ways. If not already the case, damage-resistant design will soon become no more expensive than conventional design for new buildings.

Self-Centering Steel Plate Shear Wall is an innovative damage-resistant system in which thin steel web plates dissipate the seismic energy while post-tensioned strands of connection bring the structure back to its original position to eliminate the seismic residual drift. Combination of energy dissipating of the steel web plates and self-centering of post tension strands led to a flag shape seismic behavior shown in Figure (1).

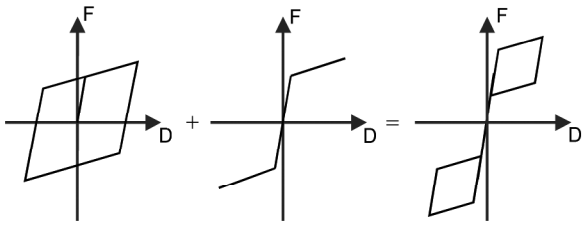

Figure 1. Seismic behavior of steel web plate and paired with self-centering connection.

2. Seismic behavior of Self-Centering Steel Plate Shear Wall

The schematic configuration of SC-SPSW is shown in Figure (2). As seen in Figure (2), the ordinary welded connections of conventional steel plate shear walls are replaced by post-tensioned connections in which post-tensioned strands run parallel through the beam and anchored at the outside of column flange, clamping beam and column together. The simple shear plate is used to resist the shear forces. The long-slotted horizontal holes of the shear tab accommodate the gap opening in the beam-column interface.

In the absence of lateral load, both beam flanges are compressed against the column by initial post-tensioned force (T_0) that equally distributed between top and bottom flange while no force generated in the web plate (Figure 3a). The initial stiffness of the post-tensioned connection is similar to that of a fully restrained connection. When the SC-SPSW is subjected to lateral force, the moment that is developed at the connection, increases the compression force (C_b) in the bottom flange and decreases the compression force (C_t) in the top flange. Shear stress also produced in the web plate, which is equivalent to two principal tension (σ_t) and compression stress (σ_c) of the same magnitude (Figure 3b).

As the lateral load rises, the top flange of beam, gradually losses the compressive force and finally decompresses from the column face (Figure 3c). At this stage, gap opening is imminent. Further rise in lateral load, opens a gap between beam and column, which results in strands elongation that provides additional stiffness and strength to resist the extra load.

Moreover, the increase of the lateral load almost immediately led to shear buckling of the web plate. After buckling, the compressive principal stresses cannot increase further and extra loads would be carried by tension field action through diagonal tensile stresses as far as full capacity of the tension field is achieved by occurring tensile yield in the web plate (Figure 3d). During unloading, assuming no compression resistance in steel plate, tensile load in the web plate decreases to zero and post-tensioned strands close the gap and bring the structure back to its initial position.

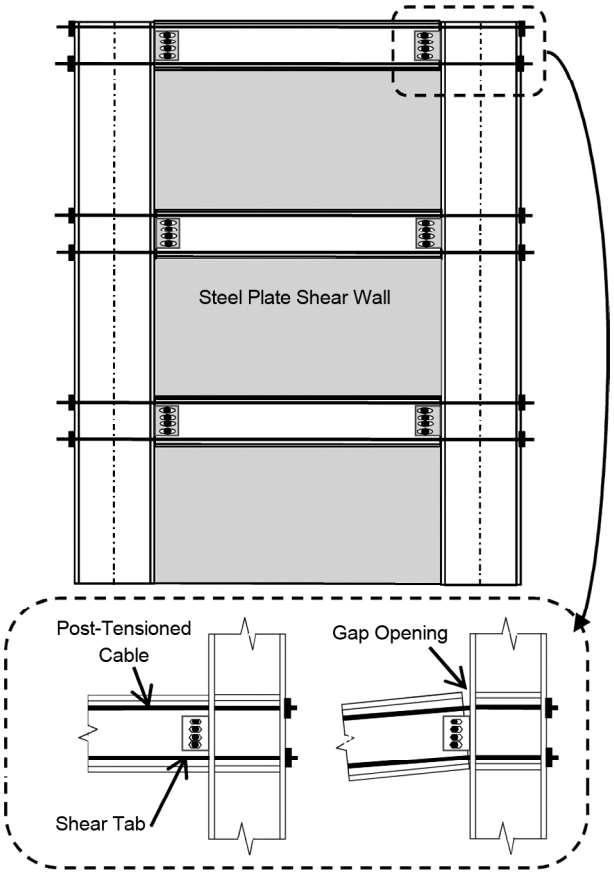

Figure 2. Self-Centering Steel Plate Shear Wall.

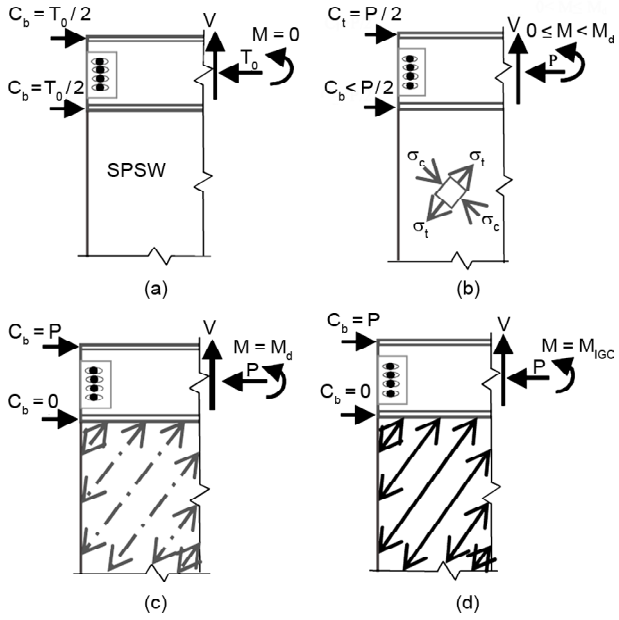

Figure 3. Self-centering connection forces.

3. SC-SPSW Archetype

Three office buildings including 5, 7 and 10 story equipped by SC-SPSW were selected to study in this paper. All the archetypes located in high seismic area (design category D_{max}). Soil classification of all archetypes belongs to site class D. The occupancy category and the importance factor of the archetypes considered as III and 1.25 respectively. The height and area of each story is 4 m and 40×48 m^2 respectively. The dead load of the floors is 500 kg/m^2. The live load of the floors is 350 kg/m^2 with the exception of live load of roof floor that is 200 kg/m^2. Tables (1) to (3) provide a summary of properties of designed archetypes. OpenSees software [12] is used for numerical simulation of the archetypes based on the study done by Arjmandzadeh and Moghadam [11].

It should be noted that the SC-SPSWs are supposed to resist the seismic force in the direction of the width of 48 m. The R-factor is considered to be 7 and it is assumed that all the required thickness of web plate is available to avoid unnecessary overstrength.

4. Time History Analysis

Nonlinear dynamic (time history) analysis was conducted for all archetypes under a suite of scaled ground motion records to investigate the seismic behavior of Self-Centering Steel Plate shear wall. Table (4) provides a summary of ground motion parameters used in the time history analysis. Each ground motion consists of a horizontal acceleration history, selected from an actual recorded event. All

Table 1. Summary of Five-Story SC-SPSW Archetypes specificatio.

	Story	HBE	HBE Weight (kg/m)	VBE	VBE Weight (kg/m)	t_w (mm)	N_S	T_0 (KN)
5 Story-Aspect Ratio = 1.5 6 shear wall Total Weight = 1127 KN	1	W30x191	284	W14x342	509	3.11	32	256
	2	W30x148	220	W14x342	509	2.88	26	231
	3	W30x148	220	W14x283	421	2.43	26	205
	4	W30x148	220	W14x283	421	1.78	20	530
	5	W30x148	220	W14x283	421	0.91	20	974

Table 2. Summary of Seven-Story SC-SPSW Archetypes specification.

	Story	HBE	HBE Weight (kg/m)	VBE	VBE Weight (kg/m)	t_w (mm)	N_S	T_0 (KN)
7 Story-Aspect Ratio = 1.5 8 shear wall Total Weight = 2021 KN	1	W30x148	220	W14x342	509	3.29	26	256
	2	W30x148	220	W14x283	421	3.17	22	231
	3	W24x131	195	W14x283	421	2.93	18	257
	4	W24x131	195	W14x283	421	2.58	14	225
	5	W24x131	195	W14x283	421	2.09	14	786
	6	W24x131	195	W14x283	421	1.48	16	1422
	7	W24x131	195	W14x283	421	0.74	18	1561

Table 3. Summary of Ten-Story SC-SPSW Archetypes specification.

	Story	HBE	HBE Weight (kg/m)	VBE	VBE Weight (kg/m)	t_w (mm)	N_S	T_0 (KN)
10 Story-Aspect Ratio = 1.5 8 shear wall Total Weight = 4426 KN	1	W33x354	527	W14x665	990	4.3	36	221
	2	W33x354	527	W14x605	900	4.22	32	199
	3	W33x354	527	W14x605	900	4.09	30	177
	4	W33x354	527	W14x426	634	3.84	28	155
	5	W30x235	350	W14x426	634	3.54	28	151
	6	W30x235	350	W14x342	509	3.14	24	126
	7	W30x148	220	W14x342	509	2.67	20	103
	8	W30x148	220	W14x342	509	2.11	14	168
	9	W30x148	220	W14x342	509	1.46	12	908
	10	W30x148	220	W14x342	509	0.71	16	693

Table 4. Summary of ground motion parameters used in time history analysis.

Earthquake					
Record Seq. No	**Vs**	**Magnitude**	**Fault Type**	**Site Class**	**Name**
326	7.1	Strike-slip	D	Duzce, Turkey	1602
309	6.7	Thrust	D	Northridge	960
356	6.7	Thrust	D	Northridge	953
354	7.3	Strike-slip	D	Landers	900
312	7.0	Thrust	D	Cape Mendocino	829
350	6.9	Strike-slip	D	Loma Prieta	767
316	6.6	Thrust	D	San Fernando	68

of the selected ground motions obtained from records of events having magnitudes and fault distance that are consistent with those that control the maximum considered earthquake.

The DBE ground motions were scaled such that the average value of the 5 percent damped response spectra for the suite of motions is not less than the design response spectrum for the site for periods ranging from 0.2 T to 1.5 T where T is the natural period of the structure in the fundamental mode for the direction of response being analyzed. The DBE ground motions were multiplied by 1.5 to achieve MCE ground motions.

Since the archetypes were analyzed under seven ground motions, the design values of member forces, member inelastic deformations and story drift are

permitted to be taken as the average of the values determined from the seven analyses at DBE and MCE ground motions.

5. Results of Time History Analysis: Inter-Story Drift

The inter-story drifts resulted from time history analysis is illustrated in Figure (4) to Figure (9).

The inter-story drifts resulted from time history analyses are illustrated in Figure (4) to Figure (9).

The 3-story and 7-story SC-SPSWs are able to meet the 2% code-based drift limit at DBE level while 10-story SC-SPSWs has slightly larger

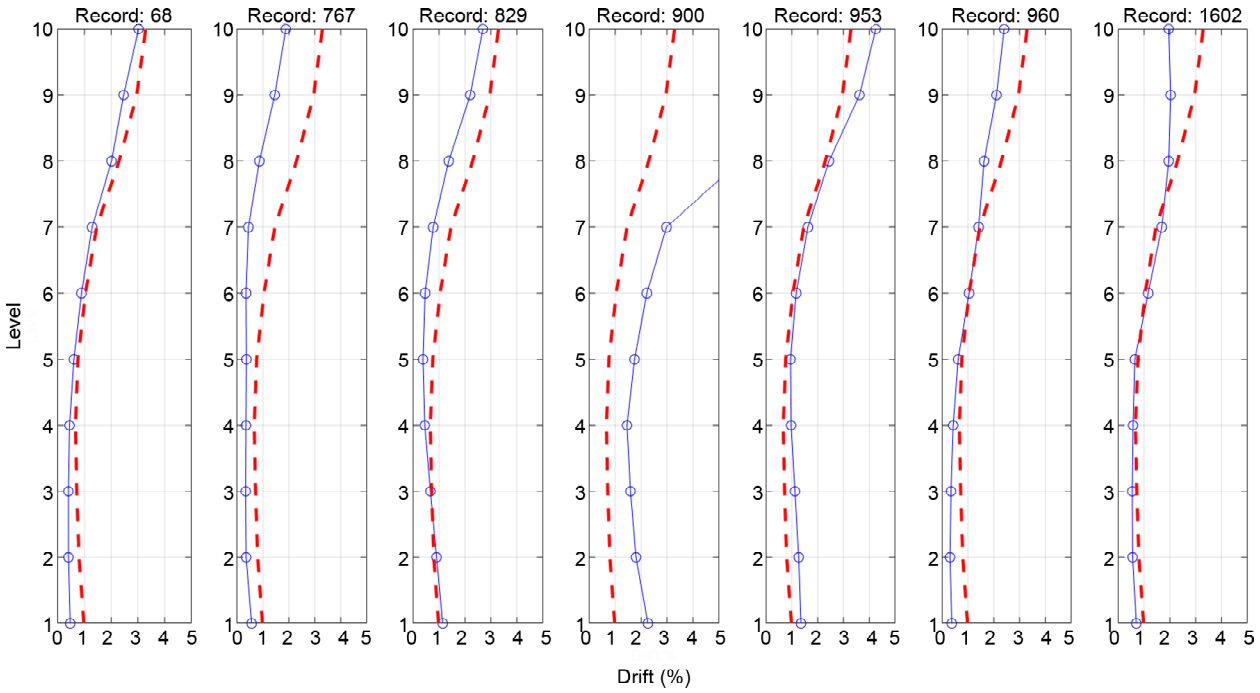

Figure 4. Interstory Drift throughout the height of 10 strory archetype at Design Based Earthquake dashed line indicates the average of Interstory Drift.

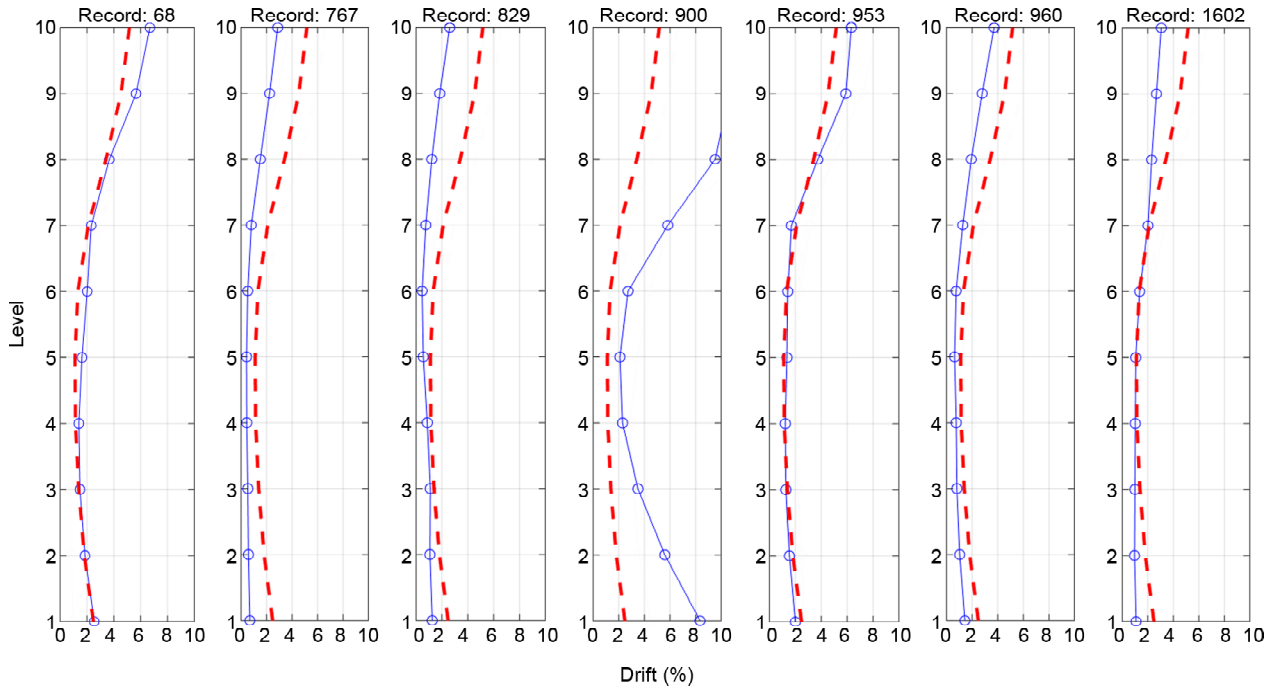

Figure 5. Interstory Drift throughout the height of 10 strory archetype at Maximum Credible Earthquake dashed line indicates the average of Interstory Drift.

inter-story drift responses in upper stories, which is caused by higher modes effect and thin web plates. As could be seen in Table (1) to Table (3), the minimum allowed thickness for web plate (6 mm according to AISC) is ignored in designing SC-SPSWs to avoid unnecessary overstrength. However, the thin web plates in upper stories resulted in huge inter-story drifts. In a practical design, the inter-story drift could be im-proved by choosing proper thickness according to AISC limits.

The 3-story and 7-story SC-SPSWs also have peak drifts less than the 4% target drift at MCE level, which resulted in conservative designs. On the other hand, the SC-SPSWs in the 10-story

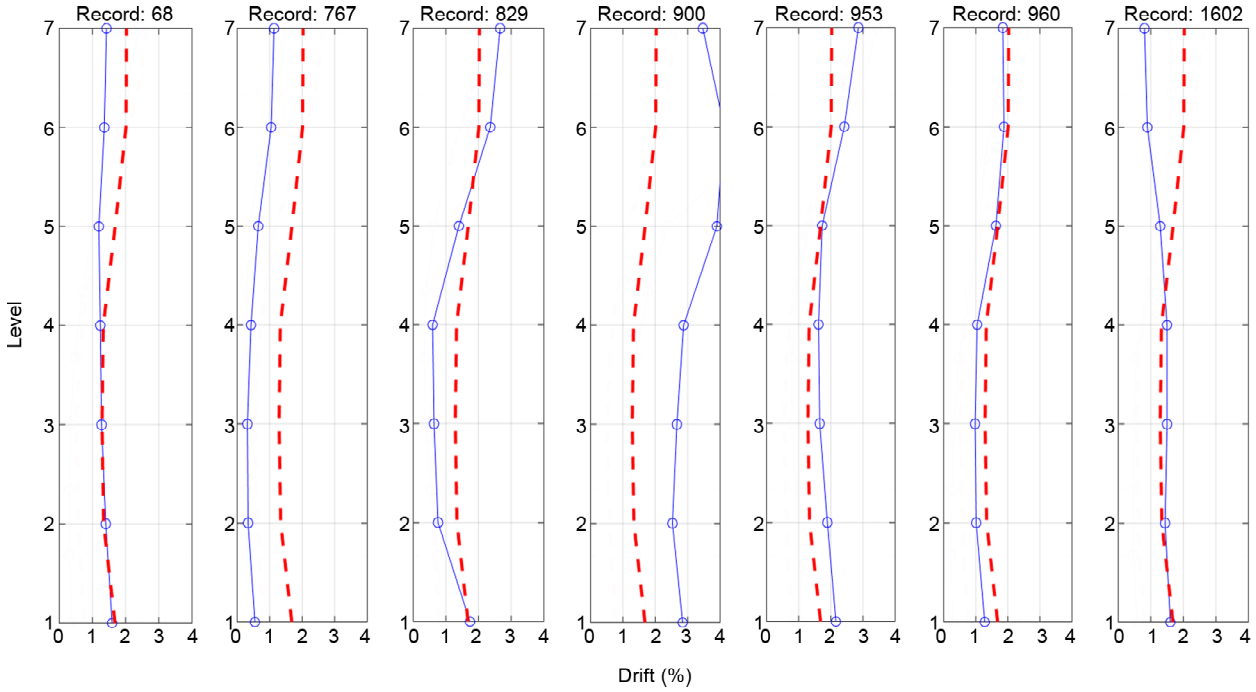

Figure 6. Interstory Drift throughout the height of 7 strory archetype at Design Based Earthquake dashed line indicates the average of Interstory Drift.

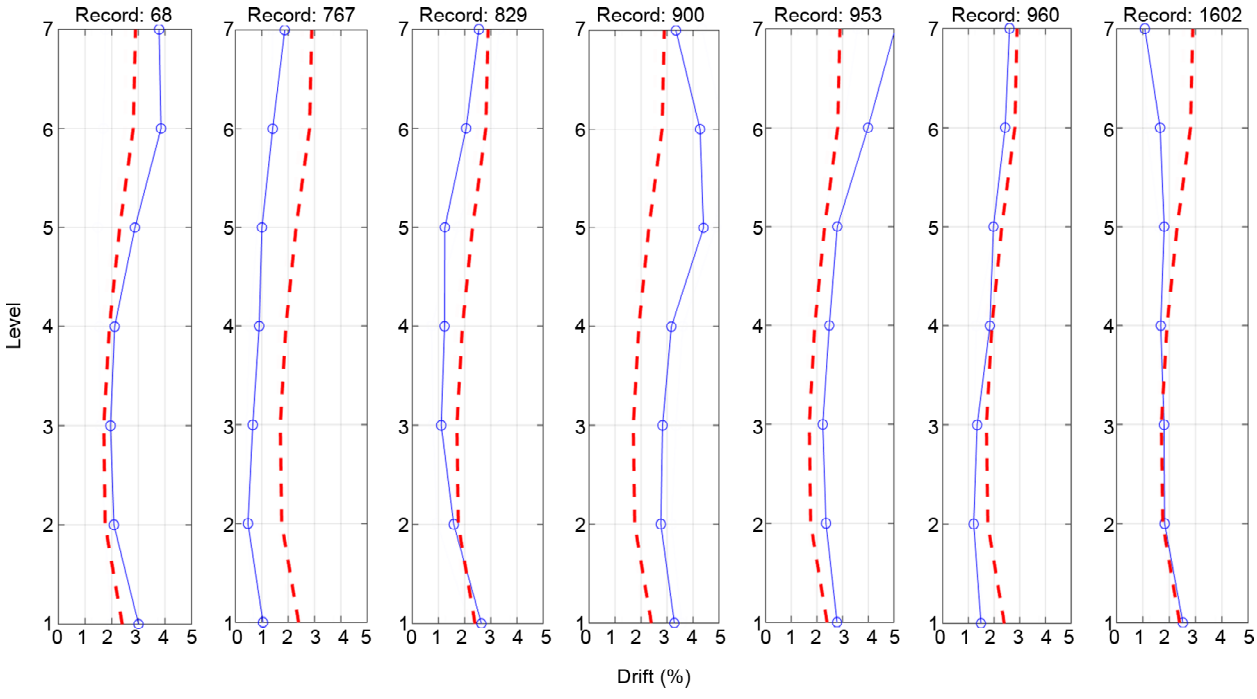

Figure 7. Interstory Drift throughout the height of 7 strory archetype at Maximum Credible Earthquake dashed line indicates the average of Interstory Drift.

archetype has larger story drifts than the 4% target drift assumed in the HBE and PT design, which meant that these walls did experience some PT and HBE yielding at MCE level. As explained above, the inter-story drift could be highly decreased by considering the minimum allowed thickness for web plate.

6. Results of Time History Analysis: Damage of Beams and Columns

Damage of HBE and VBE is measured by evaluation of the interaction equation per AISC Specifications Eqn. H1-1 [13]. The HBE and VBE damage values were used to determine the occurrence and extent of frame yielding. A

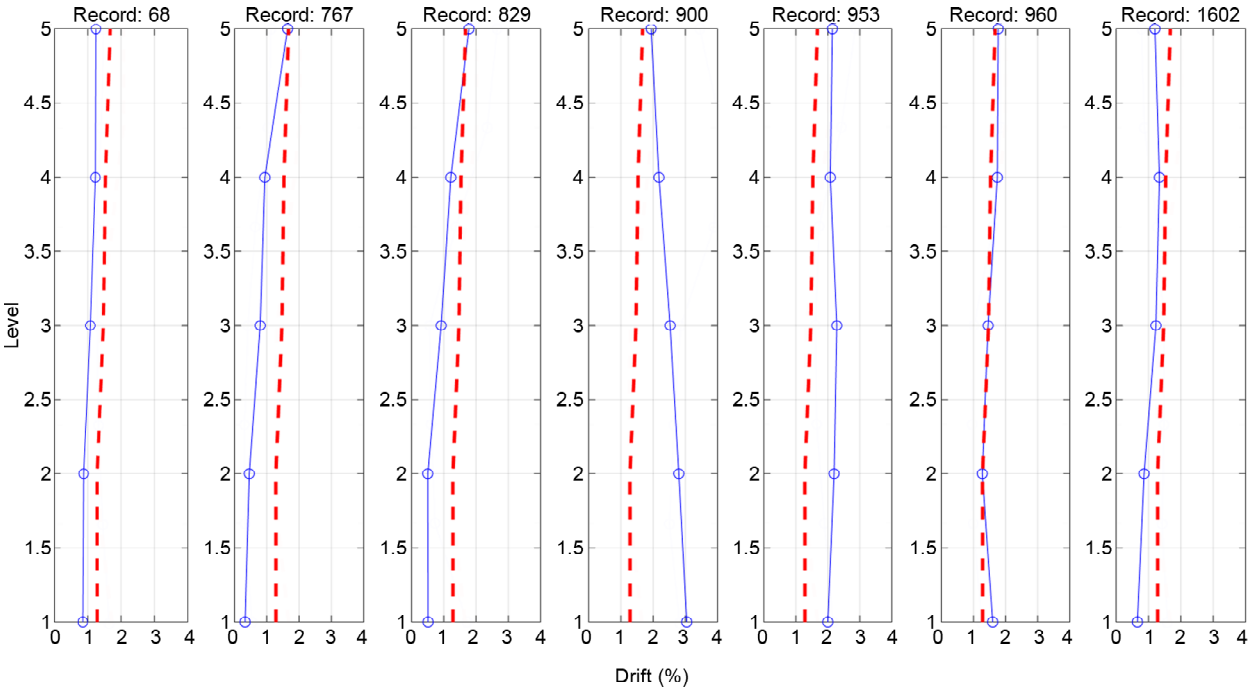

Figure 8. Interstory Drift throughout the height of 5 strory archetype at Design Based Earthquake dashed line indicates the average of Interstory Drift.

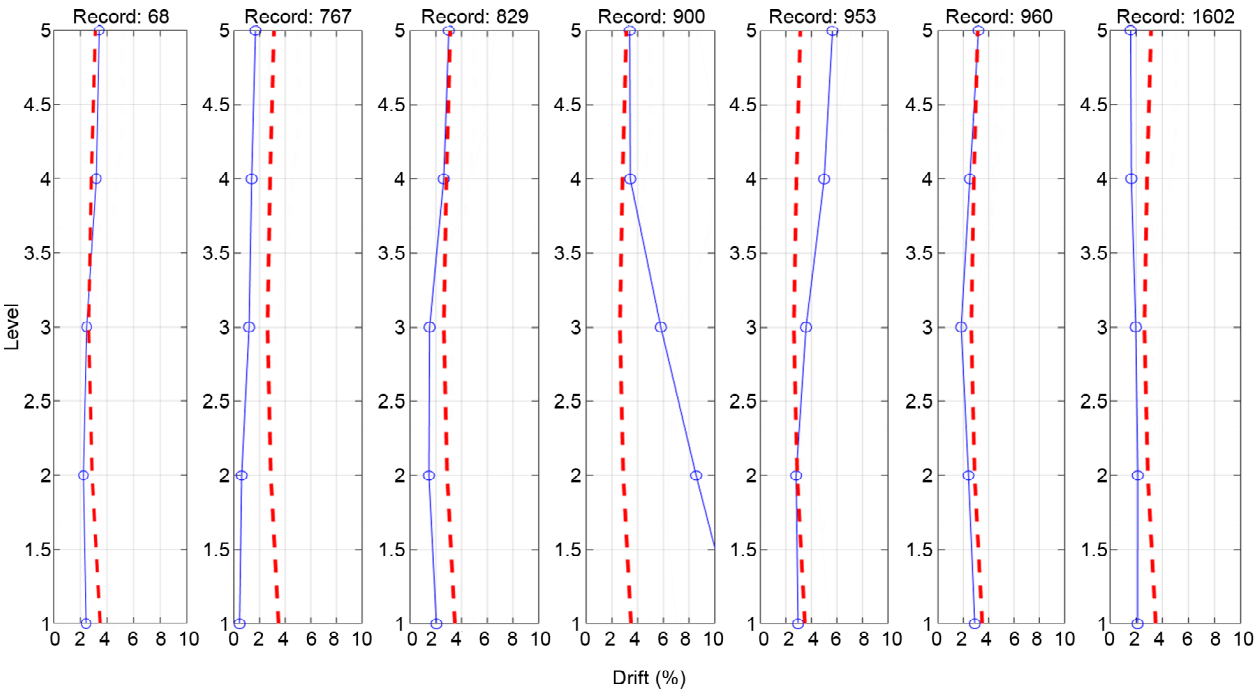

Figure 9. Interstory Drift throughout the height of 5 strory archetype at Maximum Credible Earthquake dashed line indicates the average of Interstory Drift.

damage value greater than or equal to one (1.0) indicates the combined axial flexure demand is causing significant inelastic response, and values approaching one (1.0) may also have some yielding occurring in the section.

As shown in Figure (10) to Figure (15), the HBE and VBE damages values at DBE and MCE level are well below yield thresholds with values less than 0.8, which means that the SC-SPSWs were capable to absorb and dissipate the seismic energy without any damages to beams and columns. This suggests that the proposed design procedure could be improved by using a target drift that more closely matches those observed in MCE level for these buildings, which would

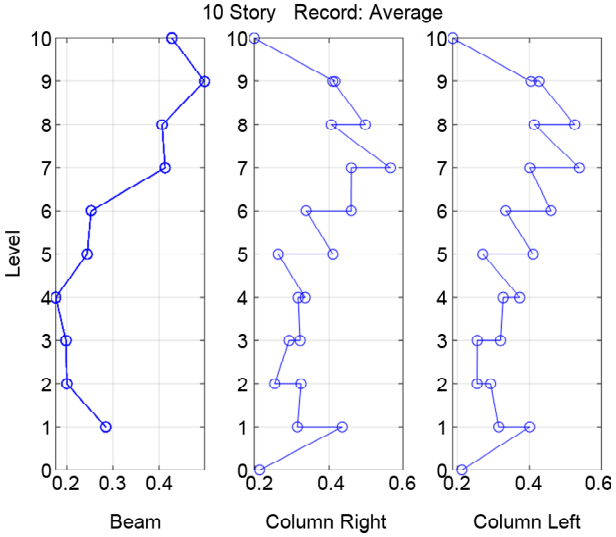

Figure 10. Average of axial and flexural stress interaction in beams and columns in 10 story archetype at Design Based Earthquake.

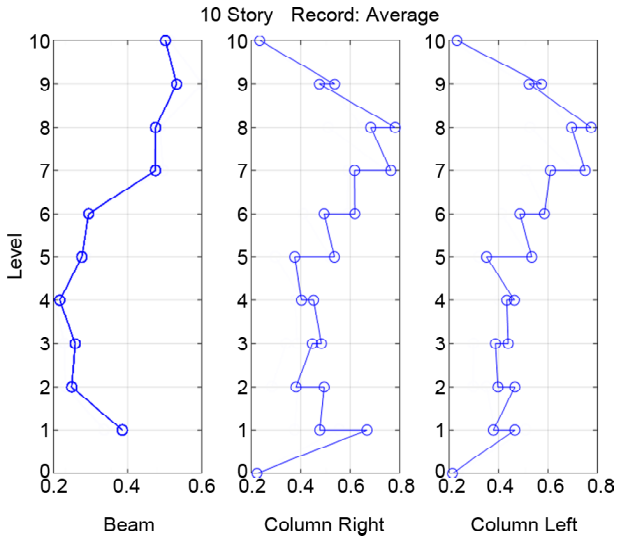

Figure 11. Interstory Drift throughout the height of 5 strory archetype at Design Based Earthquake dashed line indicates the average of Interstory Drift.

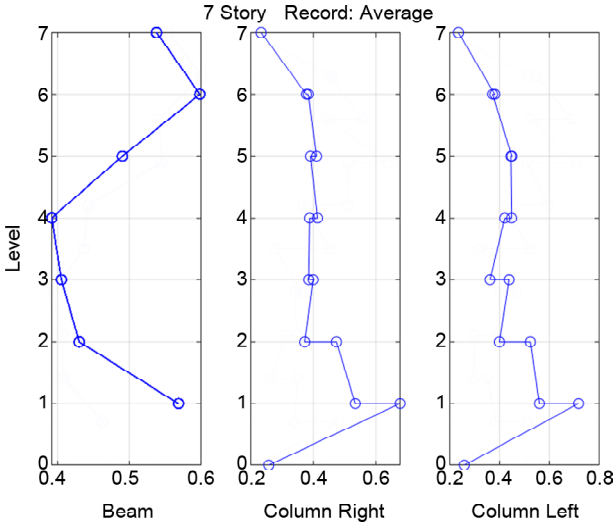

Figure 12. Average of axial and flexural stress interaction in beams and columns in 7 story archetype at Design Based Earthquake.

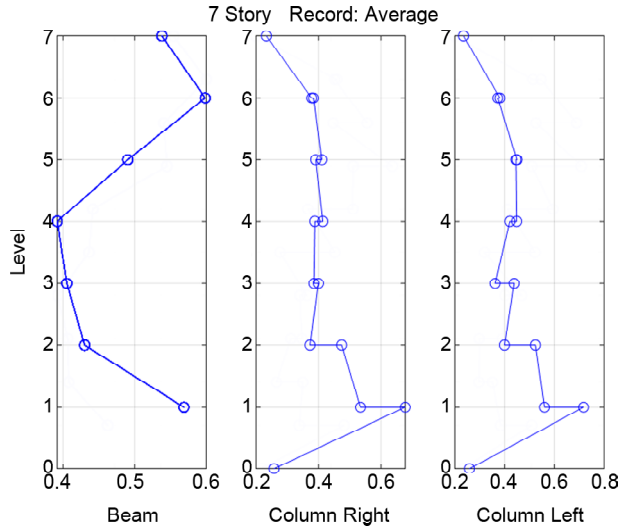

Figure 13. Average of axial and flexural stress interaction in beams and columns in 7 story archetype at Maximum Credible Earthquake.

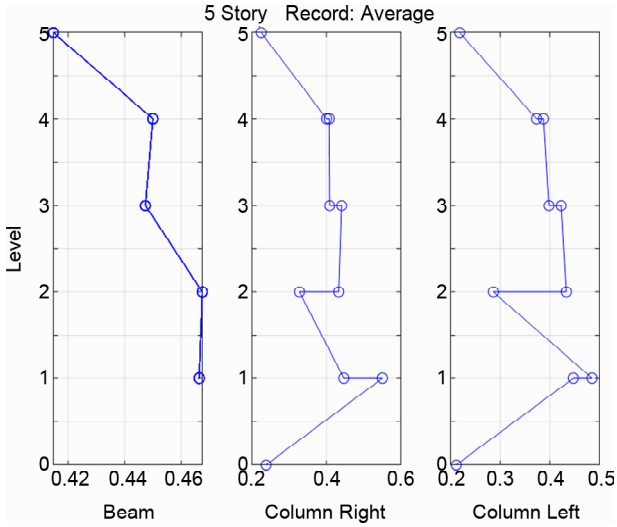

Figure 14. Average of axial and flexural stress interaction in beams and columns in 5 story archetype at Maximum Credible Earthquake.

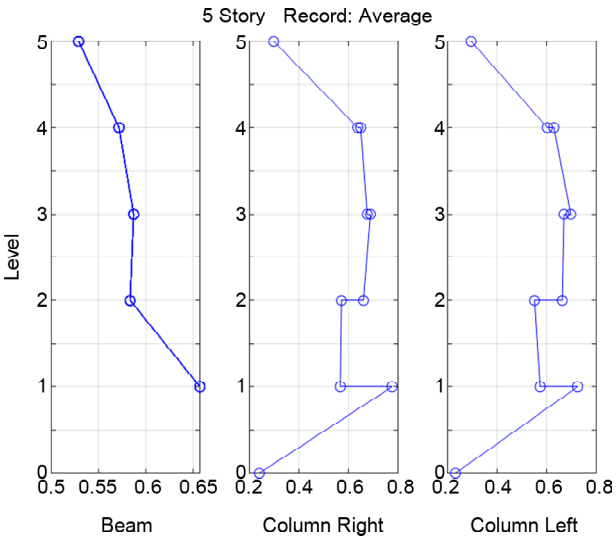

Figure 15. Average of axial and flexural stress interaction in beams and columns in 5 story archetype at Design Based Earthquake.

result in a more economical design with smaller HBE and VBE members and possibly fewer PT strands.

7. Results of Time History Analysis: Residual Drift

History of roof displacement for all the archetypes is illustrated in Figure (16) to Figure (21). The final part of each time-displacement graph represents the residual roof displacement. It should be noted that a residual story drift limit of 0.2% is used to assess recentering. Table (5) shows a summary of average values of maximum of roof displacement and roof drift. It can be seen that the SC-SPSWs were able to meet the recentering in all archetypes but as explained in previous section, some PT yielding has occurred in the archetypes, which have more than 4% inter-story drift. The question may arise: how is it possible for the archetype to recenter after experiencing PT yield?

PT yielding does decrease the recentering capabilities of the SC-SPSW, as could be seen in the archetype under record no. 900. The archetypes with PT yielding have increased residual story drifts especially at MCE level. However, PT yielding does not necessarily mean loss of collapse prevention in structural performance, because the shear connections in the HBE-to-VBE joint can adequately transfer gravity forces without the presence of PT but the connection maintains a

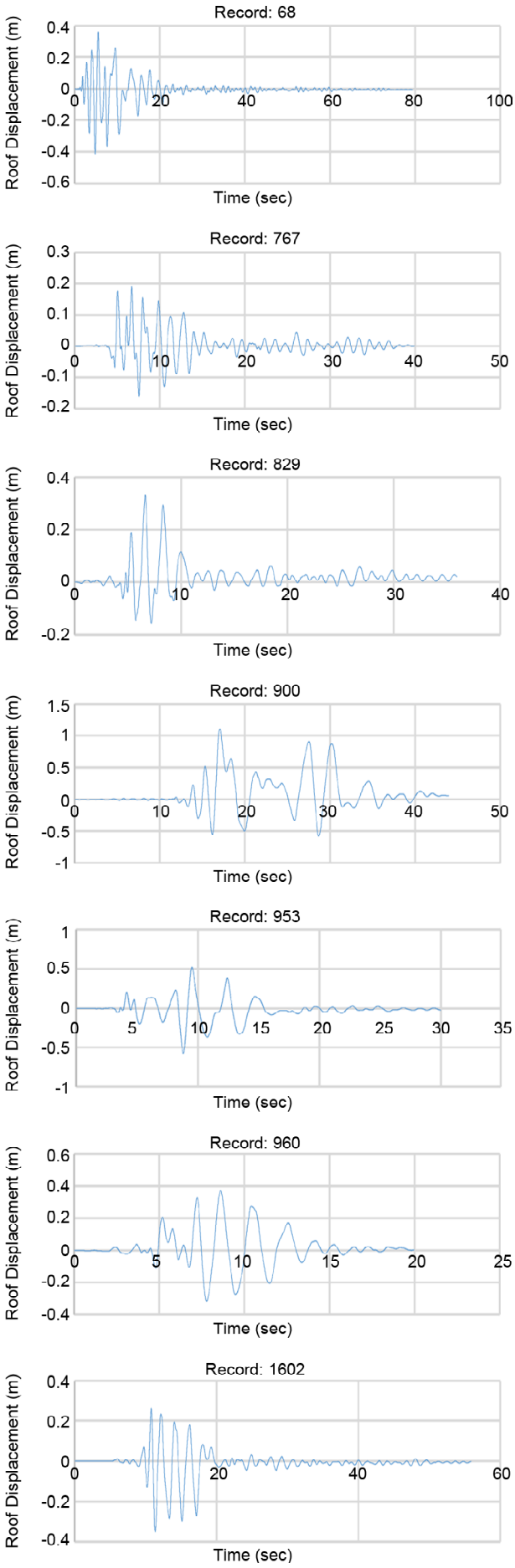

Figure 16. Roof Displacement of 10 story archetype at DBE.

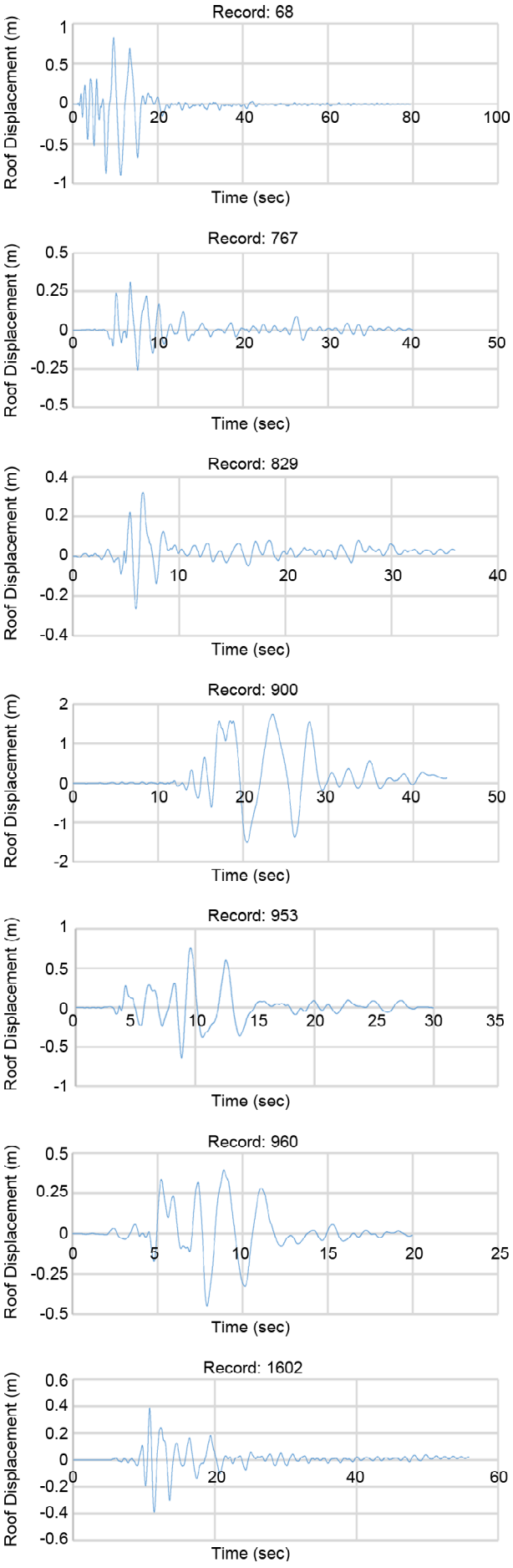

Figure 17. Roof Displacement of 10 story archetype at MCE.

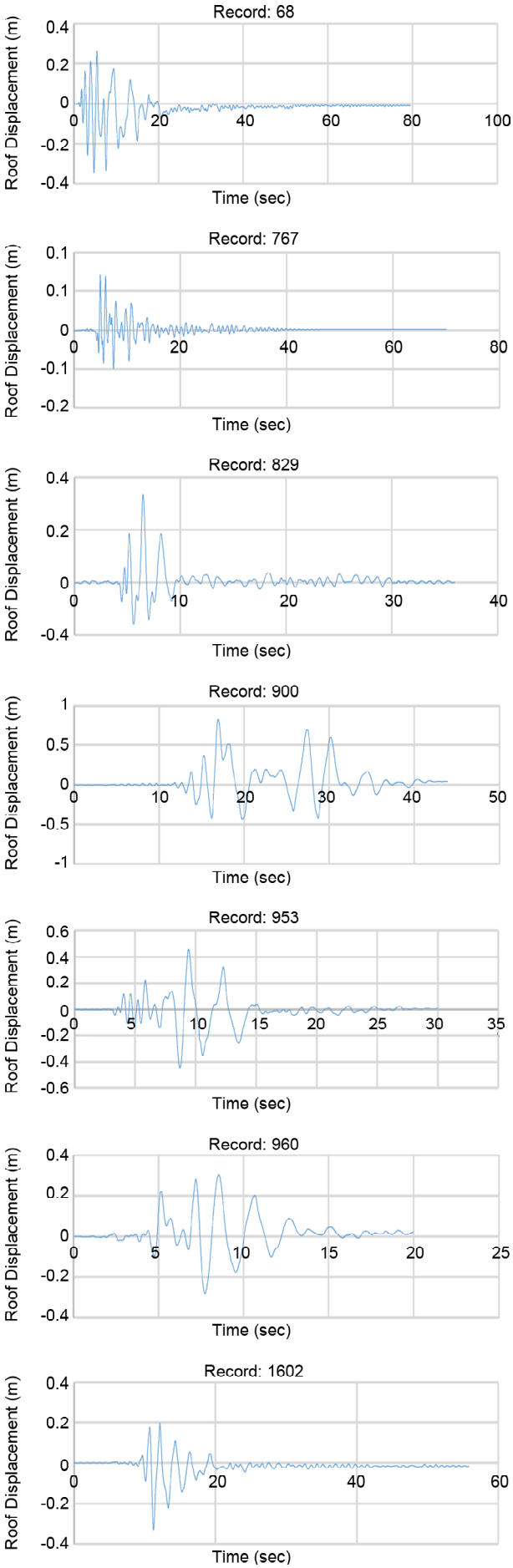

Figure 18. Roof Displacement of 7 story archetype at DBE.

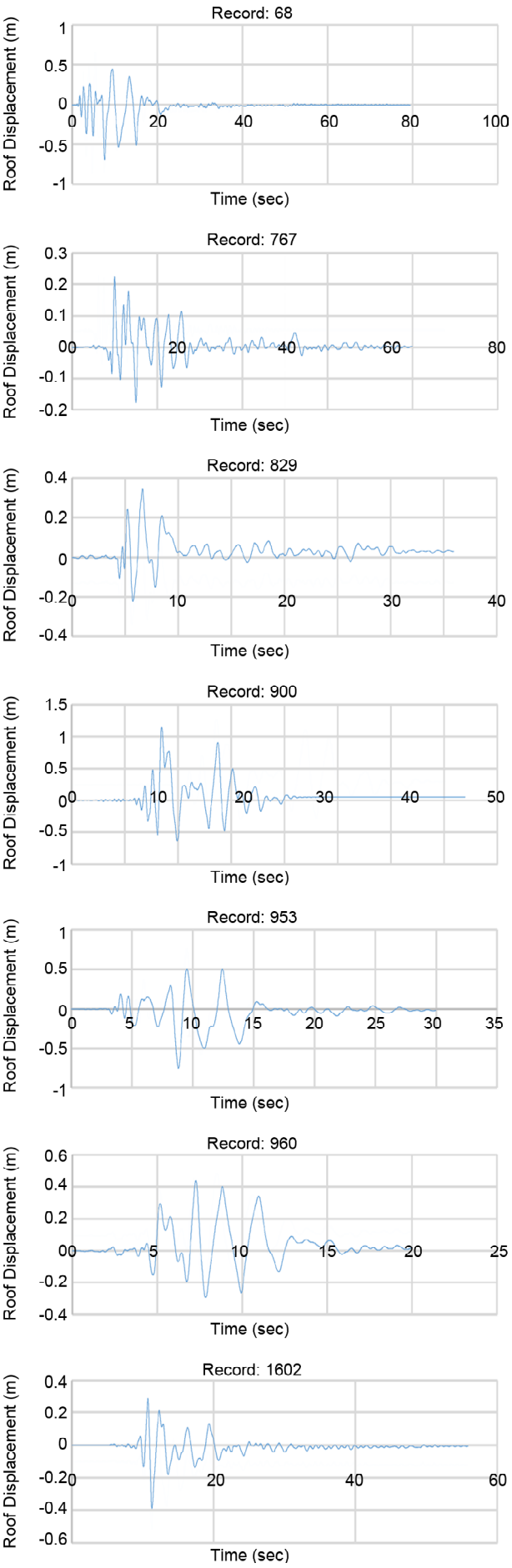

Figure 19. Roof Displacement of 7 story archetype at MCE.

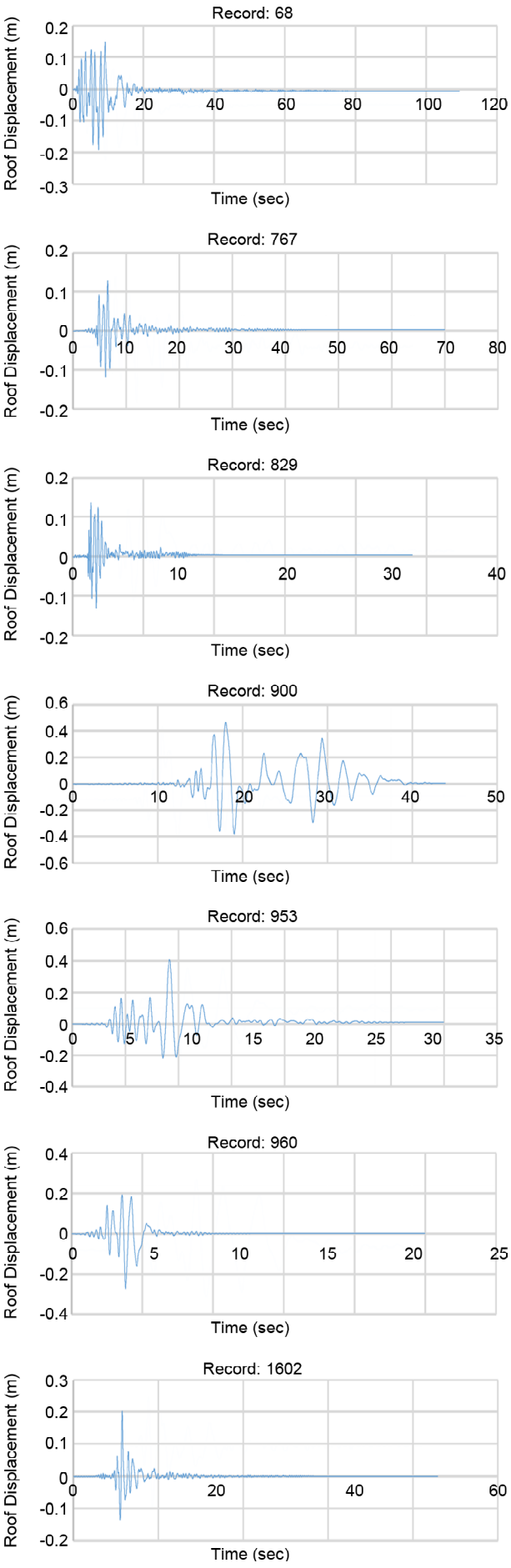

Figure 20. Roof Displacement of 5 story archetype at DBE.

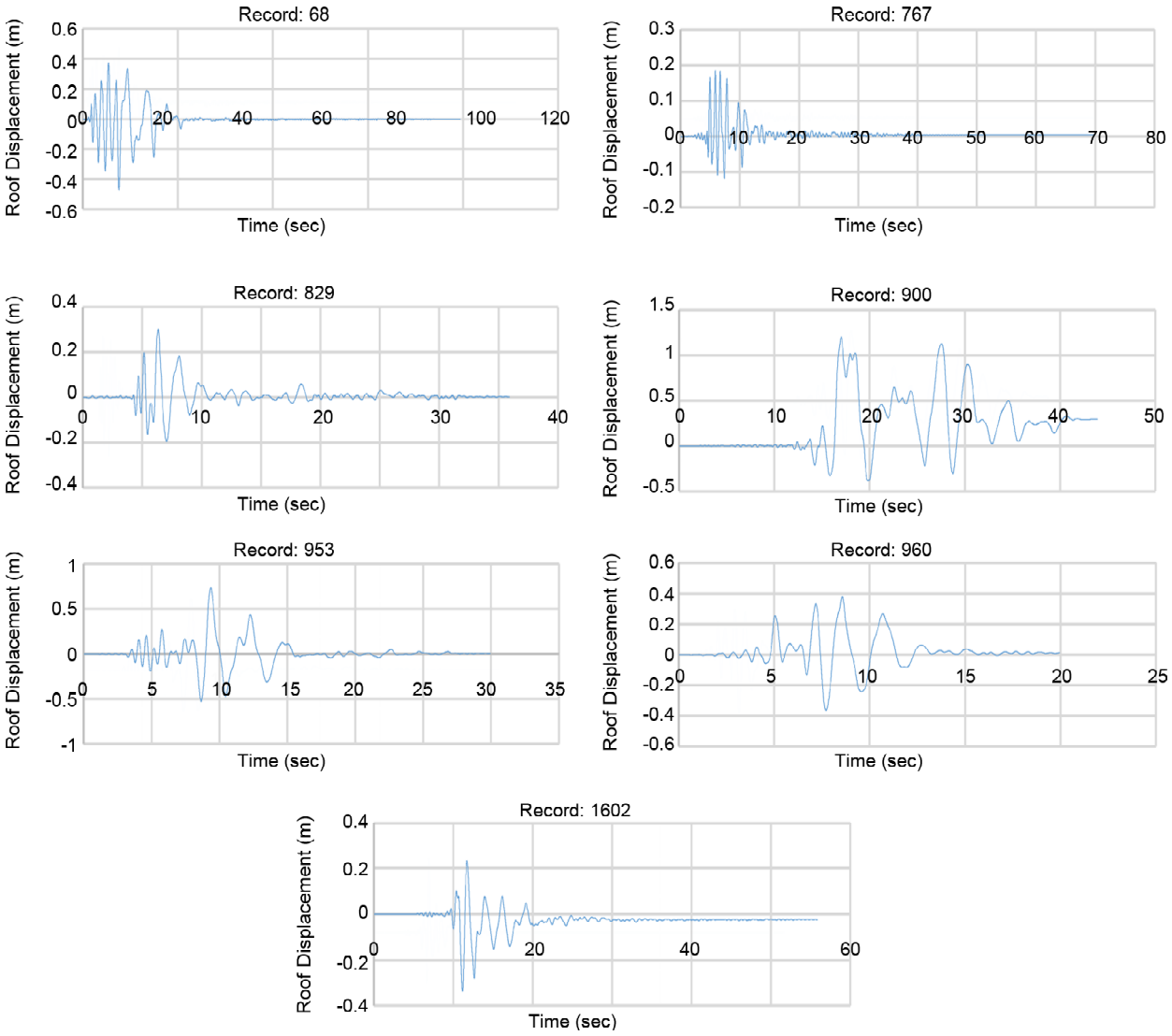

Figure 21. Roof Displacement of 5 story archetype at MCE.

Table 5. Average Roof Displacement and average Roof Drift of the archetypes at DBE and MCE.

		Maximum Roof Displacement (m)							Maximum Roof Drift (%)	Residual Roof Drift (%)
	Record Seq. No.	68	767	829	900	953	960	1602	Average	Average
DBE	10 Story	0.41	0.19	0.33	1.11	0.57	0.37	0.35	0.48	0.02
	7 Story	0.34	0.14	0.33	0.82	0.46	0.31	0.33	0.39	0.01
	5 Story	0.19	0.13	0.14	0.46	0.41	0.27	0.29	0.27	0.002
MCE	10 Story	0.89	0.31	0.33	1.74	0.76	0.44	0.39	0.69	0.12
	7 Story	0.7	0.22	0.34	1.2	0.75	0.44	0.39	0.58	0.11
	5 Story	0.47	0.18	0.3	1.2	0.74	0.38	0.34	0.52	0.2

non-zero gap rotation after unloading. However, even with HBE yielding at an individual connection and the associated increase in residual story drifts, the roof drift still recenters to a near-zero value after the earthquake and the system does not have significant loss of strength or energy dissipation.

8. Summary and Conclusion

A method of modeling SC-SPSWs was developed using a strip model for the web plates and a series of uniaxial springs for the rocking post-tensioned connections. These modeling methods were employed in the numerical models of the prototype SC-SPSW buildings. The prototype

SC-SPSW models were subjected to a suite of ground acceleration records. The results of the nonlinear dynamic analyses of the prototype SC-SPSWs showed that for mid-rise SC-SPSWs, self-centering could be achieved at DBE and MCE ground motion and seismic damage to primary element such as beams and column could be prevented. Allowed code-base drift limit could also be met if the minimum thickness of web plate would be considered in the final design.

References

1. Ricles, J.M., Sause, R., and Garlock, M.M. (2001) Post-tensioned seismic-resistant connections for steel frames. *Journal of Structural Engineering*, **127**(2), 113-121.

2. Christopoulos, C., Filiatrault, A., Uang, C.M., and Folz, B. (2002) Post-tensioned energy dissipating connections for moment-resisting steel frame. *Journal of Structural Engineering*, ASCE, **128**(9), 1111-1120.

3. Garlock, M., Ricles, J.M., and Sause, R. (2003) Cyclic load tests and analysis of bolted top and-seat angle connections. *Journal of Structural Engineering*, ASCE, **129**(12), 1615-1625.

4. Rojas, P., Ricles, J.M., and Sause, R. (2005) Seismic performance of post-tensioned steel moment resisting frames with friction devices. *Journal of Structural Engineering*, ASCE, **131**(4), 529-540.

5. Iyama, J., Seo, C-Y., Ricles, J., and Sause R. (2009) Self-centering MRFs with bottom flange friction devices under earthquake loading. *Journal of Constructional Steel Research*, **65**, 314-325.

6. Wolski, M., Ricles, J.M., and Sause, R. (2009) Experimental study of a self-centering beam-column connection with bottom flange friction device. *Journal of Structural Engineering*, ASCE, **135**(5), 479-488.

7. Lin, Y.C., Ricles, J.M., and Sause, R. (2009) Earthquake simulations on self-centering steel moment resisting frame with web friction devices. *Proceedings of the ASCE Structures Congress*, Austin, Texas.

8. Clayton, P.M. (2010) *Self-Centering Steel Plate Shear Walls: Development of Design Procedure and Evaluation of Seismic Performance*. M.Sc. Thesis, Dept. of Civil and Environmental Engineering, University of Washington, Seattle, WA.

9. Clayton, P.M. (2013) *Self-centering Steel Plate Shear Wall: Subassembly and Full-Scale Testing*. Ph.D. Dissertation, Dept. of Civil and Environmental Engineering, University of Washington, Seattle, WA.

10. Dowden. D.M. (2016) Behavior of self-centering steel plate shear walls and design considerations. *Journal of Structural Engineering*, **142**(1).

11. Arjomandzadeh, S. and Sarvghad Moghadam, R. (2022) A closer look at numerical simulation of self-centering steel plate shear walls. *Journal of Structures and Buildings*, **175**(8), 593-604, 10.1680/jstbu.19.00202.

12. Mazzoni, S., McKenna, F., Scott, M., and Fenves, G. (2009) *Open System for Earthquake Engineering Simulation User Command-Language Manual - OpenSees Version 2.0*. Pacific Earthquake, Engineering Research Center, University of California, Berkeley, CA.

13. AISC (2005b) *Seismic Provisions for Structural Steel Buildings*. ANSI/AISC 341-05, American Institute of Steel Construction, Chicago, IL.

Abbreviations

DBE: Design Based Earthquake

MCE: Maximum Credible Earthquake

SC-SPSW: Self-Centering Steel Plate Shear Wall

F: Force

D: Displacement

T_0: Initial Post Tensioned Force

C_b: Compression Force in the Bottom Flange of Beam

C_t: Compression Force in the Top Flange of Beam

σ_t: Principal Tension Stress

σ_c: Principal Compression Stress

FEMA: Federal Emergency Management Agency

AISC: Specification for Structural Steel Buildings

CSA: Canadian Standards Association

m: Meter

Kg/m^2: Kilogram per Meter Second Squared

R-factor: Response Modification Coefficient

HBE: Horizontal Boundary Element

VBE: Vertical Boundary Element

t_w: Thickness of Web Plate

N_s: Number of Strands

KN: Kilo Newton

mm: Millimeter

Kg/m: Kilogram per Meter

w_{xci}: x Components of the Distributed Loads from the Yielding Plates Acting on the Column (VBE)

w_{yci}: y Components of the Distributed Loads from the Yielding Plates Acting on the Column(VBE)

w_{xbi}: x Components of the Distributed Loads from the Yielding Plates Acting on the Beam(HBE)

w_{ybi}: y Components of the Distributed Loads from the Yielding Plates Acting on the Beam(HBE)

$R_y F_y$: Expected Yield Strength of the Plate

t_{wi}: Web Plate Thickness at Story i

α: The Angle of Tension Field Orientation

K_{strand}: Stiffness of Post-Tensioned Strands

E: Elastic Modulus of Post-Tensioned Strands

A: Area of Post-Tensioned Strands

L: Length of Post-Tensioned Strands